Numerical Simulation of Injectivity Effects of Mineral Scaling and Clay Swelling in a Fractured Geothermal Reservoir

Tianfu Xu and Karsten Pruess

Earth Sciences Division, Lawrence Berkeley National Laboratory, University of California, Berkeley, CA 94720

Abstract. A major concern in the development of hot dry rock (HDR) and hot fractured rock (HFR) reservoirs is achieving and maintaining adequate injectivity, while avoiding the development of preferential short-circuiting flow paths such as those caused by thermally-induced stress cracking. Past analyses of HDR and HFR reservoirs have tended to focus primarily on the coupling between hydrology (flow), heat transfer, and rock mechanics. Recent studies suggest that rock-fluid interactions and associated mineral dissolution and precipitation effects could have a major impact on the long-term performance of HFR reservoirs. The present paper uses recent European studies as a starting point to explore chemically-induced effects of fluid circulation in HFR systems. We examine ways in which the chemical composition of reinjected waters can be modified to improve reservoir performance by maintaining or even enhancing injectivity. Chemical manipulations considered here include pH modification and dilution with fresh water. We performed coupled thermo-hydrologic-chemical simulations in which the fractured medium was represented by a one-dimensional MINC model (multiple interacting continua), using the non-isothermal multi-phase reactive geochemical transport code TOUGHREACT. Results indicate that modifying the injection water chemistry can enhance mineral dissolution and reduce clay swelling. Chemical interactions between rocks and fluids will change a HFR reservoir over time, with some changes favorable and others not. A detailed, quantitative understanding of processes and mechanisms can suggest chemical methods for reservoir management, which may be employed to improve the performance of the geothermal system.

Key words. HFR, HDR, EGS, Mineral scaling, Clay swelling, Injectivity enhancing, Injectate mitigation, Reactive transport modeling.

1. Introduction

Flow experiments in hot fractured rock (HFR) at different field sites have provided growing evidence that chemical interactions between circulating fluids and reservoir rocks can play an important role in geothermal operations. Minerals can dissolve or precipitate in the vicinity of injection and production wells. Mineral scaling and clay swelling have very large effects on reservoir porosity, permeability, injectivity, and heat transfer characteristics.

A great deal of specific and detailed information is required to assess the chemical impact of an injection operation. The present study is not intended to represent any particular site. However, well configuration and data for mineralogical composition were taken from the European Hot Dry Rock research site (Soultz project), which situated at Soultz-sous-Forêts, northern Alsace, France (Jacquot, 2000; Durst, 2002; and Bächler, 2003). In a Hot Dry Rock (HDR) system, a well is drilled into high-temperature fractured basement rock. Then it is stimulated to enhance the natural permeability to create a reservoir into which additional wells are drilled. The European Soultz HDR project started in 1987. Two wells had been drilled to a depth of around 3500 m by 1997. A maximum downhole temperature of 165^{o}C was observed. Since production of around 200 ^{o}C fluids is more attractive for electricity generation, one of the

wells (GPK2) was re-entered and deepened to 5084 m in 1999; the measured bottom hole temperature was 200 ^{o}C.

A major concern in the development of HDR and HFR reservoirs is achieving and maintaining adequate injectivity, while avoiding the development of preferential short-circuiting flow paths that might result from phenomena such as thermally-induced stress cracking. Past analyses have tended to focus primarily on the coupling between hydrology (flow), heat transfer, and rock mechanics. Only recently have studies appeared that examine chemically-coupled effects in detail (Durst, 2002; Bächler, 2003). Results from these studies suggest that rock-fluid interactions and associated mineral dissolution and precipitation could have a major impact on the long-term performance of HFR reservoirs. The present paper uses the recent European studies as a starting point to explore chemically-induced effects of fluid circulation in HFR systems. We examine ways in which the chemical composition of reinjection waters can be modified to improve reservoir performance by maintaining or even enhancing injectivity. Chemical manipulations considered here include pH modification and dilution with fresh water.

2. Numerical Modeling Approach

2.1. Computer code

The present simulations were carried out using the non-isothermal reactive geochemical transport code TOUGHREACT, whose physical and chemical process capabilities and solution techniques have been discussed by Xu and Pruess (2001). The simulator can be applied to one-, two-, or three-dimensional porous and fractured media with physical and chemical heterogeneity, and can accommodate any number of chemical species present in liquid, gas and solid phases.

2.2 Changes of porosity and permeability

Temporal changes in porosity and permeability due to mineral dissolution and precipitation and clay swelling can modify fluid flow path characteristics. This feedback between flow and chemistry is considered in our model. Changes in porosity are calculated from changes in mineral volume fractions. Two different porosity-permeability relationships were used in the present study. The first one is a simple cubic Kozeny-Carman grain model:

$$\frac{k}{k_0} = \left(\frac{\phi}{\phi_0}\right)^3 \left(\frac{1-\phi_0}{1-\phi}\right)^2 \tag{1}$$

where ϕ is the porosity, k is the permeability (in m^2), and subscripts 0 denote initial values of variables.

Laboratory experiments have shown that modest decreases in porosity due to mineral precipitation can cause large reductions in permeability (Vaughan, 1987). This is explained by the convergent-divergent nature of natural pore channels, where pore throats can become clogged by precipitates while disconnected void spaces remain in the pore bodies. A relationship proposed by Verma and Pruess (1988), with a more sensitive coupling of permeability to porosity than the Kozeny-Carman relationship was found to better capture injectivity losses (Ontoy et al., 2003):

$$\frac{k}{k_0} = \left(\frac{\phi-\phi_c}{\phi_0-\phi_c}\right)^n \tag{2}$$

where ϕ_c is the value of "critical" porosity at which permeability goes to zero, and n is a power law exponent. Eq. (2) is derived from a pore-body-and-throat model in which permeability can

be reduced to zero with a finite ("critical") porosity remaining. Parameters ϕ_c and n are medium-dependent.

2.3. Geochemical data

A general form of rate law (Steefel and Lasaga, 1994) is used for kinetic mineral dissolution and precipitation:

$$r_m = \pm k_m A_m a_{H^+}^n \left| 1 - \frac{Q_m}{K_m} \right| \tag{3}$$

where m is the mineral index, r_m is its dissolution/precipitation rate (positive values indicate dissolution; negative values precipitation), k_m is the rate constant (moles per unit mineral surface area and unit time) which is temperature-dependent, A_m is the specific reactive surface area per kg of H_2O, a_{H^+} is the activity of H^+, and n is an empirical reaction order accounting for catalysis by H^+ in solution. K_m is the equilibrium constant for the mineral-water reaction written for the destruction of one mole of mineral m, Q_m is the ion activity product. The temperature dependence of the reaction rate constant can be expressed as

$$k = k_{25} \exp\left[\frac{-E_a}{R} \left(\frac{1}{T} - \frac{1}{298.15} \right) \right] \tag{4}$$

where E_a is the activation energy, k_{25} is the rate constant at 25 ^oC, R is the universal gas constant, and T is absolute temperature.

The parameters in the kinetic rate expression used are shown in Table 1. For most minerals, we give two sets of kinetic parameters. A reaction order n (acid catalyzed) greater than zero is used for mineral dissolution, while n = 0 (no catalysis) is used for precipitation. For minerals with only one set of the parameters with n = 0, it is used for both dissolution and precipitation.

Table 1. List of kinetic rate parameters used in Eqs. (3) and (4) for minerals considered in the present paper.

Mineral	k_{25} (moles $m^{-2}s^{-1}$)	E_a (KJ/mol)	n	Surface area (cm^2/g)
calcite	6.4565×10^{-7}	62.76	0	98×10^{-1}
	6.9183×10^{-2}	18.98	1	98×10^{-1}
quartz	1.2589×10^{-14}	87.50	0	98×10^{-1}
K-feldspar	1.0000×10^{-12}	57.78	0	98×10^{-1}
	3.5481×10^{-10}	51.83	0.4	98×10^{-1}
dolomite	1.2589×10^{-9}	62.76	0	98×10^{-1}
	1.0233×10^{-3}	20.90	0.9	98×10^{-1}
Na-smectite	1.0000×10^{-13}	62.76	0	1516×10^{-1}
	4.3652×10^{-12}	62.76	0.17	1516×10^{-1}
Ca-smectite	1.0000×10^{-13}	62.76	0	1516×10^{-1}
	4.3652×10^{-12}	62.76	0.17	1516×10^{-1}
illite	1.0000×10^{-13}	62.76	0	1516×10^{-1}
	4.3652×10^{-12}	62.76	0.17	1516×10^{-1}
pyrite	4.0000×10^{-11}	62.76	0	129×10^{-1}
galena	4.0000×10^{-11}	62.76	0	129×10^{-1}
chlorite	2.5119×10^{-12}	62.76	0	98×10^{-1}

2.4. Clay swelling

Swelling clays such as smectite and illite are layered minerals made up of negatively charged mica-like sheets, which are held together by charge-balancing interlayer cations such as Ca^{2+}, Mg^{2+}, or Na^{+} (de Siqueira et al., 1999; Tchistiakov, 2000). These cations adsorb water molecules, and water films form on clay surfaces. The increase of solution ionic strength causes reduction of the thickness of the bonded water film (shrinking). When the clay is contacted by aqueous solutions of low ionic strength, the thickness will increase and clay will swell. Using smectite as an example, this process can be schematically formulated as

$$\text{smectite} + nH_2O = \text{smectite}^{*}[\text{smectite} \bullet (H_2O)_n] \tag{5}$$

where smectite* is the swelled bulk clay with bonded water films. As water activity increases when diluting a solution of high ionic strength, the reaction (5) would be driven to the right. This will result in a decrease in bulk density of the clay, and consequently a reduction in porosity and permeability. The detailed mechanism of clay swelling (shrinking) is very complex. In the present study, we use a simple approach calculating the bulk clay density by

$$\begin{aligned} \rho &= \rho_{max}\left[1 - f_{max}\frac{I_{min} - I}{I_{min}}\right] && I < I_{min} \\ \rho &= \rho_{max} && I \geq I_{min} \end{aligned} \tag{6}$$

where ρ_{max} is the maximum clay density achieved when ionic strength I exceeds a certain minimum value I_{min}, and f_{max} is the maximum density reduction factor when I = 0. Ionic strength I is defined as

$$I = \frac{1}{2}\sum_i c_i z_i^2 \tag{7}$$

where the summation is over all aqueous species, and c_i and z_i are concentration (mol/kg H_2O) and electrical charge of species i.

3. Problem setup

3.1. Mineralogical conditions

We consider three different mineral assemblages (Table 2). The first represents strongly altered minerals from a highly fractured vein, minerals from the original granite (mainly quartz) that are fully cemented by clays, carbonates, and secondary quartz veins. The second assemblage is composed of altered granite blocks partly cemented by alteration products that consist essentially of clay minerals and carbonates, and is the most porous. The third is the unaltered granite in which the fracture density is close to zero.

3.2. Geometric configuration and fluid flow parameters

A one-dimensional MINC (multiple interacting continua) model was used (Figure 1). Subgrid 1 represents the fracture vein alteration. Subgrids 2 and 3 represent the altered and unaltered granite, respectively. The MINC method can resolve “global” flow and diffusion of chemicals in the fractured rock and its interaction with “local” exchange between fractures and matrix. Details on the MINC method for reactive geochemical transport are described by Xu and Pruess (2001).

We consider an idealized fractured porous medium with two perpendicular sets of planar, parallel fractures of equal aperture and spacing. Because of the assumed symmetry only one column of matrix blocks needs to be modeled. Our conceptual model considers a one-dimensional flow tube between injection and production well, which should be considered as a small sub-volume of a much more extensive 3-D reservoir. From the injection side to the

production side, the model consists of 72 grid blocks representing 600 m distance. The block size gradually increases from 0.1 m at the injection side to 20 m at the production side.

Table 2. Initial mineralogical composition of the three zones used in the simulations. Data were taken from Jacquot (2000), Durst (2002), and Bächler (2003). Only the total amount of smectite was reported originally. In the present simulations, Na- and Ca-smectite were distinguished and their volume percentages were assigned with 77 and 23% for Na- and Ca-smectite, respectively, according to the portion of Na^{+} and Ca^{+2} charges in water chemical composition (Table 4).

Mineral	Volume percentage of solid rock		
	Fractured vein Alteration	Altered granite	Unaltered granite
Quartz	43.9	4.09	24.2
K-feldspar		13.9	23.6
Plagioclase			42.5
Biotite			4.2
Hornblende			3.1
Chlorite		4.8	2
Calcite	4.3	3.3	0.3
Dolomite	0.7	0.8	
Illite	40.2	24.6	
Na-smectite	7.392	7.469	
Ca-smectite	2.208	2.231	
Pyrite	1	0.7	
Galena	0.3	1.3	
Other minerals (not reactive)		36.81	0.1

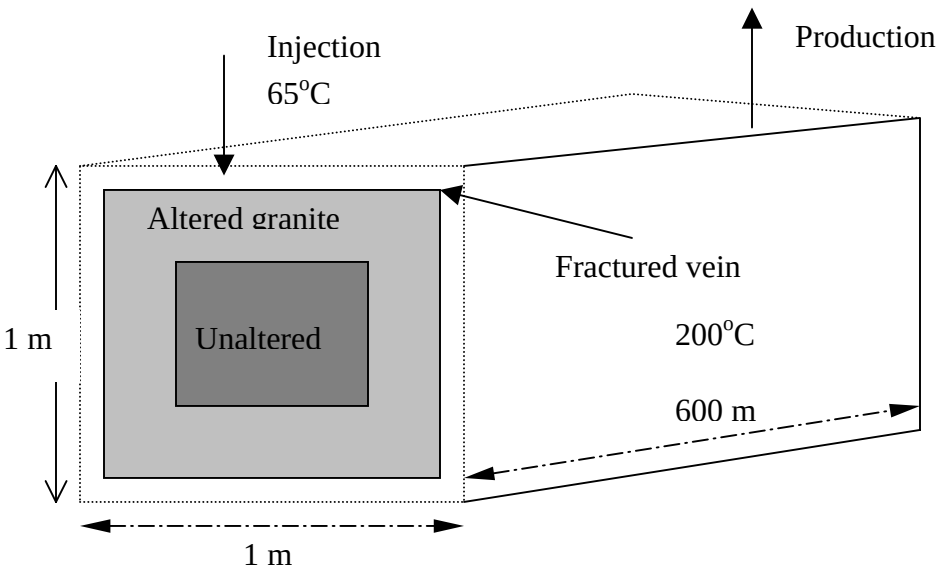

Figure 1. Subgridding of a matrix in the "multiple interacting continua" (MINC) method. The figure represents a view of a rock matrix column that is bounded by fractures.

Hydrological parameters used in the present simulations are listed in Table 3. Notice that some are different from those of Durst (2002) and Bächler (2003). For example, previous investigators used a permeability of 1×10^{-11} m^2 and a porosity of 0.1 for the fractured vein. The objective of the present study is to explore methods for minimizing mineral scaling and clay swelling, mitigating injection water chemistry, and preserving or enhancing injectivity.

Even though we took some data from the European HDR site as a starting point, we attempted to use thermophysical conditions and parameters that could represent general geothermal reservoirs. Initial reservoir temperature and pressure were 200°C and 50 MPa, respectively. An over-pressure of 2 MPa was applied to the injection (left) side. Injected water temperature was taken as 65°C. Conductive heat exchange with the surrounding low-permeability rock is an important process, and is treated with a semi-analytical technique developed by Vinsome and Westerveld (1980). In the present simulations, chemical interactions in the unaltered granite zone were not considered. This does not significantly affect chemical changes in the fractured vein because of the extremely low permeability of the granite.

Table 3. Hydrogeologic and thermal parameters used for the three mineralogical zones (a density of 2650 $kg.m^{-3}$, a heat capacity of 1000 $J.kg^{-1}$ K^{-1}, and an diffusivity of 1×10^{-9} $m^2.s^{-1}$ were used for all three zones).

Parameters	fractured vein	altered granite	unaltered granite
Volume	10%	60%	30%
Permeability (m^2)	2×10^{-12}	2×10^{-15}	2×10^{-18}
Porosity	0.2	0.1	0.02
Thermal conductivity ($W.m^{-1}$ K^{-1})	2.9	3	3
Tortuosity	0.3	0.1	0.05

3.3. Water chemistry

We started with a 165°C water sample taken from Soultz Well CPK1 at 3500 m depth (Table 4). Initial water chemical compositions for the fractured vein and altered granite zones were obtained by equilibrating the sample water with their corresponding mineral compositions (Table 2) at a temperature of 200°C.

Four types of injection waters with different chemical compositions were considered in the present simulations (Table 5). The injectate composition was not allowed to change over time. The first type corresponded to the native water in the fractured vein zone but with a lower temperature of 65°C, which should be close to the produced reservoir water without surface treatment. To understand the effects of clay (smectite and illite) swelling, we then used an injection water (Water 2) obtained by diluting Water 1 by a factor of 5 (i.e., one unit of reservoir water mixed with four units of fresh water). Carbonate scaling, especially calcite precipitation, is a significant issue for Water 2. To avoid the scaling and possibly enhance porosity and permeability, we maintained a pH of 7 by adding alkali to Water 1 and allowed sufficient time to precipitate minerals out (mainly calcite and quartz). The resulting composition is listed as Water 3 in Table 5. Water 4 was obtained by diluting Water 1 by a factor of 2 (mixing one unit of reservoir water with one unit of fresh water), and then using the same titration procedure as for Water 3.

Table 4. Initial water chemical compositions (mol/l) used in the simulations. The composition given in the second column was from a Soultz Well CPK1 sample (Durst, 2002). No measurements for Fe, Al, and Pb concentrations in the sample were reported, and small values were assumed for consistency because of the presence of minerals with these components.

		Fractured vein	Altered granite
Chemical components	Well CPK1 At 3500 depth (165^{o}C)	Equilibrium with the minerals at 200^{o}C	Equilibrium with the minerals at 200^{o}C
Ca	1.820×10^{-1}	1.810×10^{-1}	1.706×10^{-1}
Mg	4.610×10^{-3}	5.874×10^{-3}	5.540×10^{-3}
Na	1.213	1.213	1.212
K	7.180×10^{-2}	7.179×10^{-2}	9.439×10^{-2}
Fe	1.491×10^{-6}	2.191×10^{-5}	1.996×10^{-7}
Cl	1.72	1.72	1.72
SiO_2(aq)	3.500×10^{-3}	4.129×10^{-3}	4.131×10^{-3}
HCO_3	7.500×10^{-3}	7.795×10^{-3}	1.727×10^{-3}
SO_4	2.020×10^{-3}	2.062×10^{-3}	2.392×10^{-3}
Al	5.656×10^{-9}	5.655×10^{-9}	$1.518E\times10^{-6}$
Pb	1.000×10^{-12}	1.296×10^{-6}	3.391×10^{-8}
pH	5.03	5.55	5.92
I (ionic strength)	1.8834	1.8877	1.8721

Table 5. List of types of injection waters with different chemical compositions (mol/l) at 65^{o}C temperature used in the simulations.

Injection water	Water 1	Water 2	Water 3	Water 4
Chemical component	Initial fractured vein water (with different T)	Diluting Water 1 by a factor of 5	Equilibrating Water 1 with fractured vein mineralogy at 65^{o}C and pH=7	Diluting Water 1 by a factor of 2, followed by the same titration procedure as Water 3.
Ca	1.810×10^{-1}	3.620×10^{-2}	1.715×10^{-1}	8.587×10^{-2}
Mg	5.874×10^{-3}	1.175×10^{-3}	7.853×10^{-3}	4.010×10^{-3}
Na	1.213	2.426×10^{-1}	1.213	6.065×10^{-1}
K	7.179×10^{-2}	1.436×10^{-2}	7.180×10^{-2}	3.589×10^{-2}
Fe	2.191×10^{-5}	4.382×10^{-6}	1.511×10^{-6}	7.892×10^{-7}
Cl	1.72	3.440×10^{-1}	1.72	8.600×10^{-1}
SiO_2(aq)	4.129×10^{-3}	8.258×10^{-4}	5.064×10^{-4}	5.066×10^{-4}
HCO_3	7.795×10^{-3}	1.559×10^{-3}	$2.490E\times10^{-4}$	3.419×10^{-4}
SO_4	2.062×10^{-3}	4.124×10^{-4}	2.020×10^{-3}	1.010×10^{-3}
Al	5.655×10^{-9}	1.131×10^{-9}	5.209×10^{-10}	1.546×10^{-9}
Pb	1.296×10^{-6}	2.592×10^{-7}	1.342×10^{-10}	1.826×10^{-11}
pH	5.55	5.96	7	7
I (ionic strength)	1.888	0.378	1.865	0.933

3.4. Simulation setup

A total of six simulations were performed using different combinations of over-pressure at the injection side, porosity-permeability (ϕ-k) relationship, clay swelling, and injection water chemistry, as summarized in Table 6. In the first simulation an over-pressure of 2 MPa, a simple cubic Kozeny-Carman ϕ-k relationship (Eq. 1), and injection Water 1 (the "base case") was used. To demonstrate the effect of higher over-pressure on injectivity, Simulation 2 used a value of 5 MPa. Other conditions and parameters were not changed from the base case. We called this the "over-pressure simulation".

Simulation 3 used the Verma and Pruess ϕ-k relationship of Eq. 2 ("Verma-Pruess simulation"). This relationship requires two parameters, one is the "critical" porosity ϕ_c, and another is n, a power law exponent. In the present simulations, we simply used a ϕ_c of 0.16 (80% of initial porosity of 0.2 for the fractured vein), and an n of 2. A ϕ_c of 80% initial porosity is quite reasonable and may be conservative. A permeability experiment of Moore et al. (1983), in which a heated aqueous fluid was passed down a temperature gradient through Westerly Granite, showed a reduction in permeability of 96% with an 8% reduction of the initial porosity over a two-week period.

Simulation 4 used Water 2 (one unit of reservoir with four units of fresh water). The native reservoir water has an ionic strength (I) equal to1.8834, the diluted injection water has an I of 0.37755. The minimum ionic strength I_{min} (Eq. 6) to maintain clay density is dependent on the type of clays, type of salts dissolved in water, and temperature and pressure conditions. In the present simulations, we simply select I_{min} = 1.5, which is slightly below the I of the native reservoir water. The maximum density reduction factor f_{max} is also a predetermined parameter. Experiments on compacted bentonite showed that density could be reduced due to swelling by 26% (JNC, 2003). Studies conducted by Newman (1987) and de Siqueira et al. (1999) indicated that the layer spacing in dry clays is about 9.8 Å. If one assumes that the diameter of a water molecule is 2.7 Å, clay hydrates containing one, two, and three molecular layers of water will have a spacing of around 12.5, 15.2 and 17.9 Å. In the reservoir, the clay may not be well contacted by the injected water and conditions could be different from the lab. We used a maximum density reduction factor f_{max} = 5%. We called this the "swelling simulation".

Simulation 5 injected Water 3 that was obtained by precipitating minerals out under pH 7 conditions. The purpose is to avoid carbonate scaling and potentially enhance porosity and permeability by mineral dissolution. We called this simulation the "pH 7" simulation.

Simulation 6 injected Water 4 that is similar to Water 3 but mixed with fresh water (1:1, "mixing simulation"). This water has a I of 0.93315 (below 1.5 of the I_{min}), and slight clay swelling will occur.

Table 6. List of simulations with different combinations of over-pressure, porosity-permeability relationship, clay swelling, and injection water chemistry.

Simulation	Over-pressure at injection	ϕ-k relationship	Clay swelling	Injection water chemistry
1 (base case)	2MPa	Kozeny-Carman		Water 1 (see Table 5)
2 (over-pressure)	5MPa	Kozeny-Carman		Water 1
3 (Verma-Pruess)	2MPa	Verma-Pruess		Water 1
4 (swelling)	2MPa	Verma-Pruess	f_{max} = 5%	Water 2
5 (pH 7)	2MPa	Verma-Pruess	f_{max} = 5%	Water 3
6 (mixing)	2MPa	Verma-Pruess	f_{max} = 5%	Water 4

4. Results and discussion

The injection rates over time obtained from the six different simulations are presented in Figure 2. By increasing the over-pressure at the injection point from 2 to 5 MPa, initially the injection rate is proportionally increased (compare Simulations 2 and 1). After five years, the temperature at the production side decreases to below 200^{o}C due to the larger injection rate. By using the Verma-Pruess ϕ-k relationship instead of Kozeny-Carman in the base case, the injection rate decreases faster due to a larger permeability reduction (compare Simulations 3 and 1). After ten years, the injection rate declines to 0.16 kg/s from the initial 0.4 kg/s

By considering clay swelling (Simulation 4) using a 1:4 diluted injection water, the injection rate dramatically decreases to 0.1 kg/s in several months. Clay swelling contributes to a porosity decrease of 0.016. Later, decreases in the injection rate occur due to mineral scaling. After five years, the injection rate is close to zero. In actual field operation, the injection would stop before that.

By using pH 7 injection water (Simulation 5) —minerals such as calcite have been already precipitated out, the injection rate gradually increases to 0.52 kg/s at ten years from the initial 0.4 kg/s, which enhances injectivity. At ten years, the temperature at the production side just reaches 200^{o}C due to the enhanced injection rate.

Simulation 6 uses a similar pH 7 injection water as the previous case but diluted 1:1 by mixing it with fresh water. This water has an intermediate I of 0.93315 compared to the swelling simulation with I = 0.3776. The clay swelling causes a slight porosity decrease close to 0.01. This reduces the injection rate to about 0.25 from the initial 0.4 kg/s, a reduction that is considerably less than the 0.1 kg/s obtained in Simulation 4 (swelling). Similar to the previous simulation, the diluted pH 7 water also causes dissolution effects and enhances injectivity. The injection rate then increases linearly with time after the clay swelling stops. The rise of permeability is similar to that in Simulation 5. After ten years, the rate reaches about 0.35 kg/s, close to the initial value. This suggests that modifying the injection water could avoid mineral scaling and enhance injectivity. Mitigation is achieved by adding alkali to maintain a higher pH and letting minerals (mainly calcite and quartz) precipitate out prior to reinjection. Further reviewing Figure 2, we can see that injection rates in Simulations 1 and 2 decrease with time and the injection rate vs. time curves have negative slopes even though Simulation 2 applied a much higher over-pressure.

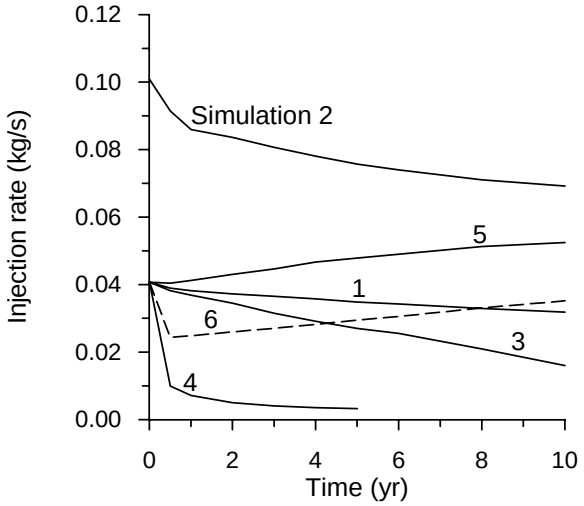

Figure 2. Injection rate (kg/s) over time of the fracture-matrix column with an area of 1 m^2 obtained from different simulations. Simulation 1: base case; 2: over-pressure; 3: Verma-Pruess; 4: swelling; 5: pH 7; 6 mixing.

Changes in porosity are due to mineral dissolution and precipitation, and clay swelling. Porosity increases indicate that mineral dissolution is dominant (Figure 3), while porosity decreases when precipitation dominates. Changes in permeability (Figure 4) are calculated by changes in porosity using Eq. 1 or 2.

Now let us examine the changes of mineral abundances. For Simulations 1-3, the 65^{o}C injection water is over-saturated with quartz and under-saturated with respect to calcite because this water was in equilibrium with reservoir rock at 200^{o}C. Therefore, quartz is gradually precipitating due to kinetics (Figure 5a). A precipitation peak can be observed because the precipitation rate increases with temperature. Later along the flow path quartz starts to dissolve because as the temperature of the injectate increases quartz tends to be under-saturated again. In reality, the injected water would first precipitate amorphous silica. The use of quartz rather than amorphous silica in the simulation doesn't affect the results because both minerals have the same chemical composition (SiO_2).

Significant calcite dissolves close to the injection side because calcite solubility decreases with temperature (Figure 6a), which is different from quartz. Calcite has a higher solubility at the injection temperature of 65^{o}C. As temperatures increase away from the injection point, calcite becomes over-saturated and precipitation occurs. Areas of calcite dissolution and precipitation move gradually away from the injection point due to changes in temperature along the flow path. A maximum of 3.6% volume of calcite has been precipitated after ten years, which is more than one order of magnitude larger than the amount of quartz deposited. Notice that amounts of calcite and quartz precipitation and their distribution depend on their precipitation kinetics.

Dolomite also dissolves close to the injection side but later precipitates. The amounts of dolomite precipitation are about one order of magnitude smaller than calcite. Some pyrite and galena precipitation, and very slight illite and smectite precipitation occurs near the injection point.

For the swelling simulation (Simulation 4), precipitation of calcite and quartz is more localized due to the lower injection and the faster temperature increase with distance. For the two pH 7 simulations (Simulations 5 and 6), calcite dissolution occurs constantly throughout the distance and time. The lower temperature (65^{o}C) injection water is just saturated in terms of calcite. Along the flow path, temperature increases and pH decreases (Figure 7a), causing competing effects on calcite solubility. The effect of pH plays a more important role than temperature for calcite, giving rise to calcite dissolution. Quartz also dissolves continually because both higher temperature and lower pH are favorable for quartz dissolution. A maximum of quartz dissolution is close to 2%, which is comparable to calcite dissolution (close to 3%). On the other hand, dolomite precipitation occurs constantly along the flow path and throughout time with a maximum value of 2.3%. Overall dissolution is dominant and porosity increases.

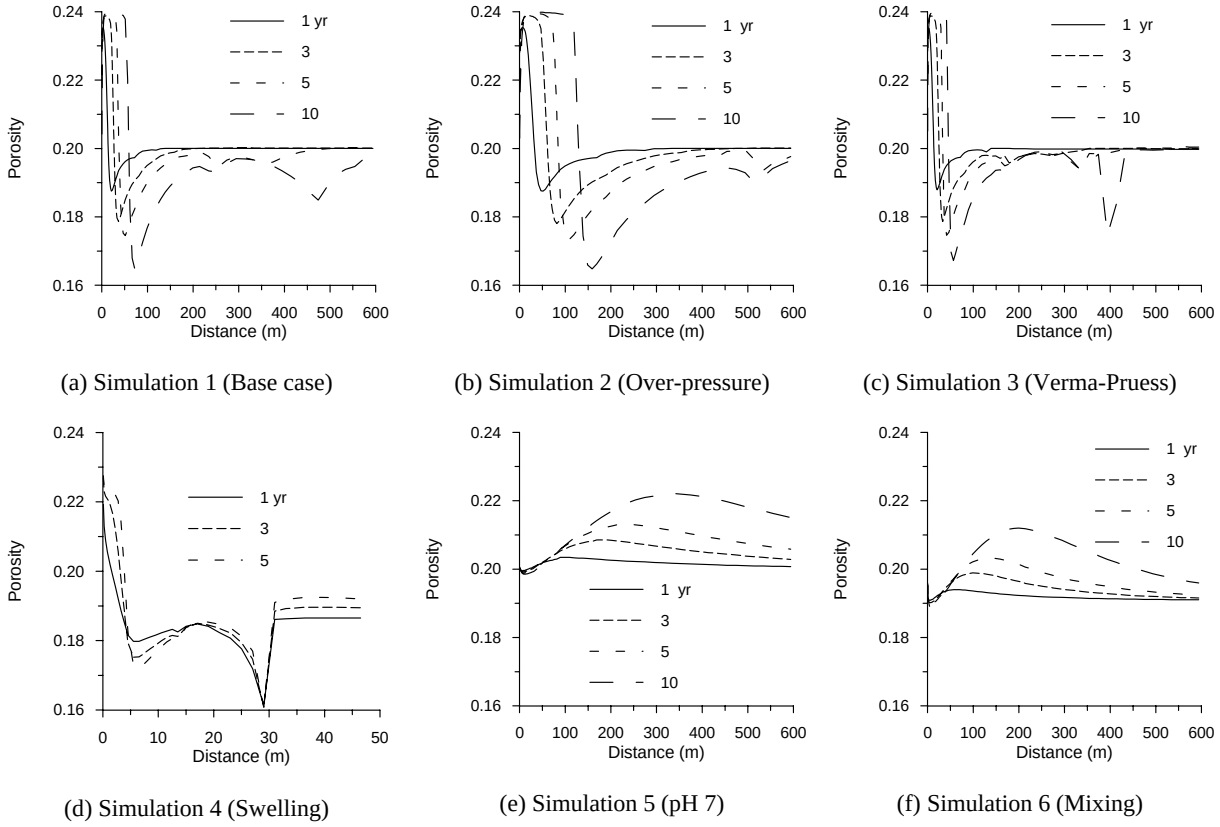

(a) Simulation 1 (Base case) (b) Simulation 2 (Over-pressure) (c) Simulation 3 (Verma-Pruess)

(d) Simulation 4 (Swelling) (e) Simulation 5 (pH 7) (f) Simulation 6 (Mixing)

Figure 3. Distribution of porosity obtained from all six different simulations.

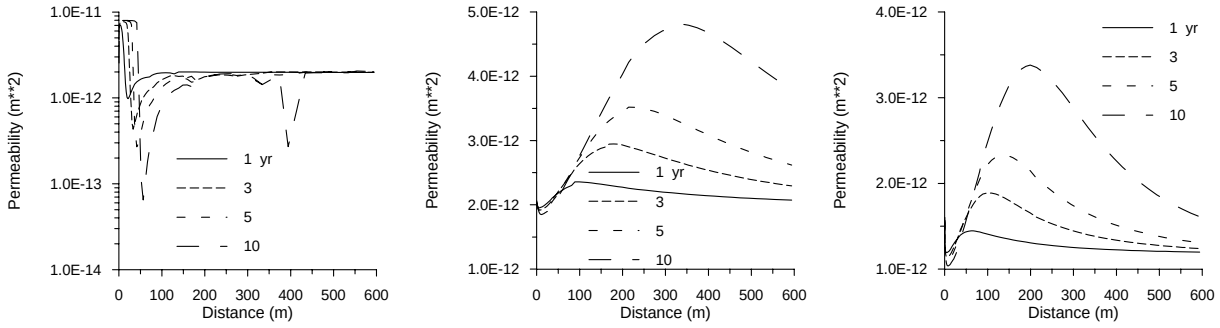

(a) Simulation 3 (Verma-Pruess) (b) Simulation 5 (pH 7) (c) Simulation 6 (Mixing)

Figure 4. Distribution of permeability obtained from three different simulations.

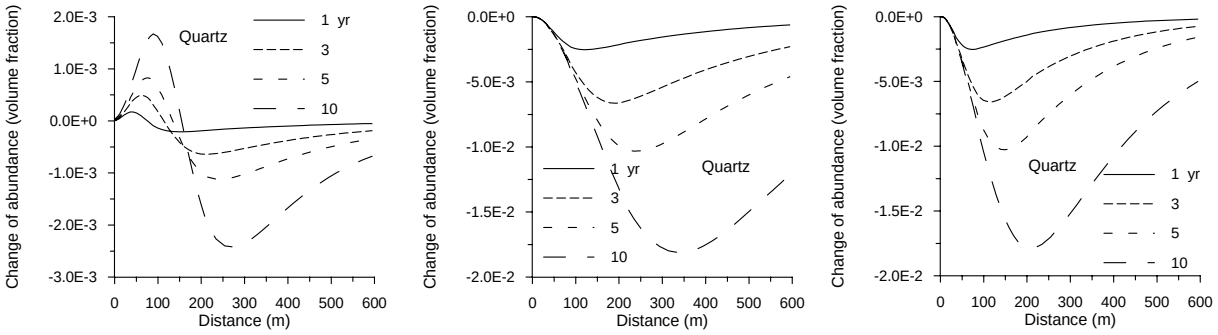

(a) Simulation 3 (Verma-Pruess) (b) Simulation 5 (pH 7) (c) Simulation 6 (Mixing)

Figure 5. Changes of quartz abundance (given in reservoir volume fractions) obtained from three simulations.

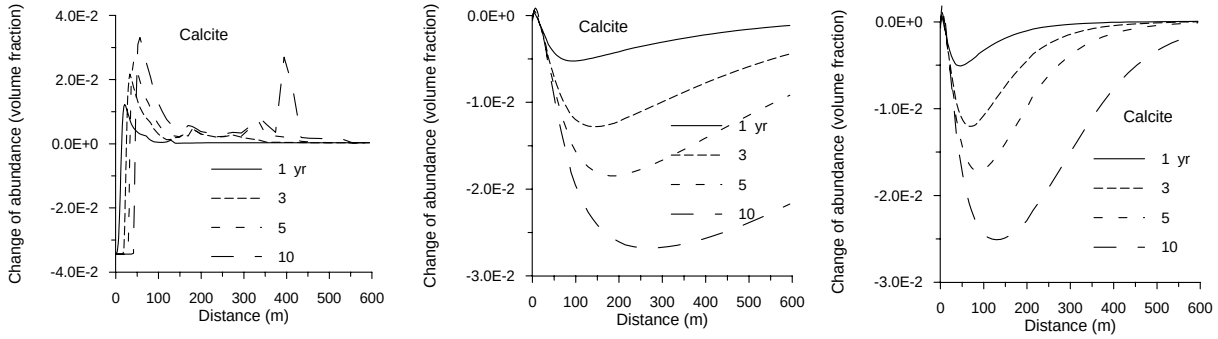

(a) Simulation 3 (Verma-Pruess) (b) Simulation 5 (pH 7) (c) Simulation 6 (Mixing)

Figure 6. Changes of calcite abundances (given in reservoir volume fractions) obtained from three simulations.

Now we return to the pH distribution along the flow path (Figure 7a). The higher pH 7 water eventually will displace the lower pH native reservoir water if the rock matrix was not considered in the simulation. The higher H^+ concentration in the matrix diffuses into the fractures, maintaining lower pH at distances. The rock matrix also buffers temperature in the main flow channel at the fracture walls (Figure 7b). If diluted water is injected, the matrix also buffers solute concentrations in the fracture and keeps higher ionic strength (I). However, the buffering capability for I is limited to initial times only, unlike for pH and temperature. The MINC model with rock matrix subgridding as used in the present simulations is an important tool for representing these different fracture-matrix interactions.

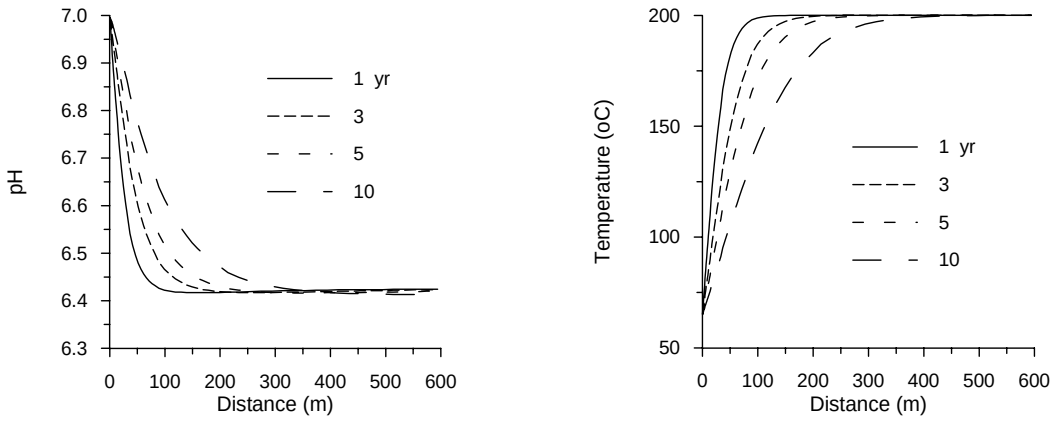

(a) pH (b) Temperature

Figure 7. Distribution of pH and temperatures obtained from the mixing simulation (Simulation 6).

5. Summary and Conclusions

Injecting produced geothermal brines directly back into the reservoir results in mineral scaling (especially calcite). The reinjected highly concentrated water from the geothermal reservoir can maintain clay density without swelling, but this limits the availability of water for injection. Mixing the produced geothermal water with large amounts of fresh water (1:4) can cause serious clay swelling when it is reinjected.

Modifying the injection water could avoid mineral scaling and enhance injectivity. Mitigating injection water chemistry could be an efficient way to achieve this objective. Hydrological approaches such as applying a high over-pressure at the injection well cannot solve the scaling problem. In this work, we added alkali to maintain a higher pH and let minerals (mainly calcite and quartz) precipitate out. Using this modified injection water results in the injection rate gradually increasing because of continual calcite and quartz dissolution. By mixing the reservoir water with appropriate amounts of fresh water (1:1), together with adding alkali to let minerals precipitate out, clay swelling could be reduced and injectivity be maintained.

The higher pH injection water is not able to simply displace the lower pH native reservoir water because of the buffering effect of the rock matrix. Therefore, the MINC model considering rock matrix subgridding as used in the present simulations is very important for modeling realistically pH and temperature buffering in the fractures.

The reaction kinetics of mineral alteration and the relationship between porosity and permeability changes are uncertain. Sensitivity studies should be performed in the future. The well configuration and data for mineralogical composition in this study were taken from the European HDR research site, but the results and conclusions should be useful for other HFR reservoirs, because calcite and quartz are commonly present in geothermal systems.

Chemical interactions between rocks and fluids will change a HFR reservoir over time, with some changes favorable and others unfavorable. A detailed, quantitative understanding of processes and mechanisms are needed to develop reservoir management tools based on geochemistry. Such novel approach should result in improvements in reservoir performance.

Acknowledgements. We are grateful to Marcelo Lippmann and Guoxiang Zhang for a review of the manuscript and suggestions for improvement. This work was supported by the Assistant Secretary for Energy Efficiency and Renewable Energy, Office of Geothermal Technologies, of the U.S. Department of Energy, under Contract No. DE-AC03-76SF00098.

References

Bächler, D., 2003. Coupled thermal-hydraulic-chemical modeling at the Soultz-sous-Forêts HDR reservoir (France). PhD dissertation, Swiss Federal Institute of Technology, Zurich, Switzerland.

de Siqueira, A.V., Lobban, C., Skipper, N.T., Williams, G.D., Soper, A.K., Done, R., Dreyer, J.W., Humphreys, R.J., and Bones, J.A.R., 1999. The structure of pore fluids in swelling clays at elevated pressures and temperatures. J. Phys.: Condens. Matter 11, 9179-9188.

Durst, D., 2002. Geochemical modeling of the Soultz-sous-Forêts Hot Dry Rock test site: Coupled fluid-rock interaction to heat and fluid transport. PhD dissertation, Université de Neuchâtel, France.

Jacquot, E., 2000. Modéllisation thermodynamique et cinétique des reactions géochimiques entre fluids de basin et socle cristalline. Application au site experimental du programme européen de recherché en géothermie profonde (Soultz-sous-Forêts, Bas Rhin, France). PhD dissertation, Univ. Louis Pasteur, Strasbourg, France.

JNC (Japan Nuclear Cycle Development Institute), 2003. Repository Design and Engineering Technology. Technical Report.

Malmstrom M., Banwart S., Lewenhagen J., Duro L., and Bruno J., 1996. The dissolution of biotite and chlorite at 25ºC in the near-neutral pH region. Contaminant Hydrology, 21, 201-213.

Moore, D. E., Morrow, C. A., and Byerlee, J. D., 1983. Chemical reactions accompanying fluid flow through granite held in a temperature gardient. Geochimica et Cosmochimica Acta, 47, 445-453.

Newman, A.C.D., 1987. Chemistry of Clays and Clay Minerals (London: Mineralogical Society)

Ontoy, Y., Molling, P. L., Xu, T., Spycher, N., Parini, M. and Pruess, K., 2003. Scaling of hot brine injection wells: supplementing field studies with reactive transport modeling. In Proceedings of TOUGH Symposium 2003, Lawrence Berkeley National Laboratory, Berkeley, California, May 12–14.

Steefel, C.I., and Lasaga, A.C., 1994. A coupled model for transport of multiple chemical species and kinetic precipitation/dissolution reactions with applications to reactive flow in single phase hydrothermal system. Am. J. Sci. 294, 529-592.

Tchistiakov, A.A., 2000. Physico-chemical aspects of clay migration and injectivity decrease of geothermal classic reservoirs. Proceedings of World Geothermal Congress, Kyushu-Tohoku, Japan, May 28 – June 10, 2000, 30873095.

Vaughan, P.J., 1987. Analysis of permeability reduction during flow of heated, aqueous fluid through Westerly Granite, in C.F. Tsang (ed.), Coupled processes associated with nuclear waste repositories, 529-539, Academic Press, New York.

Verma, A., and Pruess, K., 1988. Thermohydrological conditions and silica redistribution near high-level nuclear wastes emplaced in saturated geological formations. J. Geophys. Res., 93, 1159-1173.

Vinsome, P. K. W., and Westerveld, J., 1980. A simple method for predicting cap and base rock heat losses in thermal reservoir simulators. J. Canadian Pet. Tech., 19 (3), 87–90.

Xu, T., and Pruess, K., 2001. Modeling multiphase non-isothermal fluid flow and reactive geochemical transport in variably saturated fractured rocks: 1. Methodology. Am. J. Sci., 301, 16-33.